



City Research Online

City, University of London Institutional Repository

Citation: McNamara, A. M. & Taylor, R.N. (2004). The influence of enhanced excavation base stiffness on prop loads and ground movements during basement construction. *The Structural Engineer*, 82(4), pp. 30-36.

This is the accepted version of the paper.

This version of the publication may differ from the final published version.

Permanent repository link: <https://openaccess.city.ac.uk/id/eprint/8067/>

Link to published version:

Copyright: City Research Online aims to make research outputs of City, University of London available to a wider audience. Copyright and Moral Rights remain with the author(s) and/or copyright holders. URLs from City Research Online may be freely distributed and linked to.

Reuse: Copies of full items can be used for personal research or study, educational, or not-for-profit purposes without prior permission or charge. Provided that the authors, title and full bibliographic details are credited, a hyperlink and/or URL is given for the original metadata page and the content is not changed in any way.

City Research Online:

<http://openaccess.city.ac.uk/>

publications@city.ac.uk

THE INFLUENCE OF ENHANCED EXCAVATION BASE STIFFNESS ON PROPPING LOADS AND GROUND MOVEMENTS DURING BASEMENT CONSTRUCTION

A.M.McNamara

Research Fellow, City University, London.

R.N.Taylor

Professor of Geotechnical Engineering, City University, London.

SYNOPSIS

The use of piles installed beneath deep excavations as a means of enhancing the stiffness of the soil and so reducing the spread of movements to the surrounding ground has been investigated. Experimental data were obtained from a series of plane strain centrifuge model tests undertaken at 100g in which three different formation base stiffnesses were modelled. The tests were able to simulate the stress changes that result from the complex propping and excavation sequence associated with top down basement construction. Reductions in horizontal loads of the order of 30% were found when piles were introduced to stiffen the ground beneath excavation formation level. Additionally, significant reductions in heave at the base of the excavation led to overall reductions in both horizontal and vertical ground movements behind the retaining wall. The number of piles was found to have a strong influence on the magnitude of reduction in ground movement, especially with increasing time after completion of the simulated excavation.

INTRODUCTION

Control of movements around deep basement excavations during construction is known to be highly dependent upon the design of the perimeter wall and the excavation and propping sequence adopted. Over the years new techniques such as the use of embedded retaining walls have been developed that have both hastened the operations involved in construction and also enabled much greater control of local ground movements in the area behind the retaining wall. However deep seated movements associated with heave in the ground below the excavation formation have, in general, remained unaddressed. The use of heave resisting piles aimed at minimising deep-seated movements beneath an area to be excavated and thereby reducing ground movements outside an excavation is a relatively recent innovation and the effectiveness of such measures cannot yet be quantified accurately by finite element analysis. In this paper the results of a series of centrifuge model tests¹ are described in which three different formation stiffnesses were modelled. These were achieved by carrying out a series of reference tests in which the formation was unstiffened followed by two series of tests which included either one or two rows of cast in situ piles installed before excavation beneath the excavation formation level. The use of such piles led to both reductions in ground movement and significant reductions in prop loads.

The plane strain model apparatus was capable of simulating the stress changes associated with excavation of a twelve metre deep prototype. The tests involved the use of apparatus that included three levels of propping used to support a very stiff retaining wall and enabled

realistic simulation of a basement excavation incorporating top down construction techniques. The magnitude of prop loads was determined from changes in oil pressure in the hydraulic system. A schematic representation of the apparatus is shown in Figure 1.

PRINCIPLES OF CENTRIFUGE MODELLING

Accurate physical modelling requires the model to be subjected to stresses that are representative of those in a similar prototype. This is because soil behaviour is governed by stress level and stress history, and, as a consequence, there is a need to model in situ stresses that change with depth to reproduce both strength and stiffness aspects of soil behaviour. This can be achieved, in a small scale model, by applying an elevated equivalent gravitational field using the inertial radial acceleration field produced by a geotechnical centrifuge. In the model, centrifuged self weight stresses increase with depth from zero at the surface to values that are determined by the soil density and the applied radial acceleration field. Such physical modelling also offers opportunities to correlate to other analyses and this is achieved by carrying out a series of tests with known and repeatable boundary conditions and parameters.

It is important to subject the centrifuge model to a similar stress history as that in the corresponding prototype situation. If the soil in the model and prototype have the same density then, for a model of dimensional scale 1:N of the prototype, the requirement of

stress similarity means that the vertical stress at depth $h_{m(\text{odel})}$ should be the same as at $h_{p(\text{rototype})}$ where

$$h_p = N h_m \quad (1)$$

This is achieved by accelerating the model (of dimensional scale 1:N) at N times Earth's gravity using a centrifuge which then conveniently gives stress similarity at homologous points throughout the model. Newton's Laws of motion state that in pulling a mass out of its straight flight path around a curve of constant radius, r (m), the centrifuge will impose a radial acceleration (towards the centre of rotation) of a (m/sec^2) where

$$a = \omega^2 r \quad (2)$$

where ω = angular velocity (radians/second).

The model will experience an equal and opposite force towards the base of the model, and thus the requirement is for:

$$ma = mNg \quad (3)$$

where m = unit mass of soil in the model and prototype, N = gravity scaling factor, g = acceleration due to gravity ($9.81\text{m}/\text{s}^2$). The effect of the radial acceleration is therefore to increase the effective self weight of the model. Consequently, it follows that, with care, models can be made with stress profiles that closely resemble a corresponding prototype when subjected to an acceleration field in the centrifuge as indicated in Figure 2. Errors in the stress level in the model exist because a non-uniform acceleration field is created in the centrifuge owing to the fact that the radius, r , increases with model depth. However, this error is limited to about 3%. Care is taken to ensure that the model is orientated such that horizontal stresses caused by the use of flat, rather than cylindrical surfaces are also

minimised.. Further details on the principles of centrifuge modelling are given by Schofield² and Taylor³.

The geotechnical centrifuge at City University

The Acutronic 661 centrifuge⁴ used by the Geotechnical Engineering Research Centre at City University is shown schematically in Figure 3. The swinging platform at one end of the rotor has overall dimensions of 500mm x 700mm with a usable height of 500mm. A package weight of up to 400kg at 100g or 200kg at 200g can be accommodated, making the centrifuge a 40g/tonne machine. The package is balanced by a 1.45 tonne counterweight that can be positioned, along the centrifuge arm, in advance of a test by a screw mechanism. The radius to the swinging platform is 1.8m giving a working radius of between 1.5m and 1.6m, requiring an operating speed of approximately 240rpm to give 100g at 1.55m radius.

Electrical and hydraulic connections are available at the swinging platform and are supplied through a stack of slip rings. 55 slip rings are electrical and 5 fluid with 15 bar capacity. Of the electrical slip rings 5 are used to transmit transducer signals, which are converted from analogue to digital by the on-board computer and may be amplified prior to transmission in bits. The remaining slip rings are used for communicating closed circuit television signals, supplying power for lights or operating solenoids or motors as necessary. The fluid slip rings may be used for water, oil or compressed gas.

THE MODEL AND APPARATUS

The tests were carried out at 100g which means, from the scaling laws previously explained, that 10mm at model scale is equivalent to 1000mm at prototype scale and that stress similarity can be achieved between prototype and model when a 1:100 scale model is subject to 100g. The model was prepared from speswhite kaolin that was consolidated, in an aluminium strongbox, from a slurry of 120% water content. The strongbox had a series of herringbone pattern drainage channels machined into the base that were connected to the clay sample through a porous plastic sheet. Connection of a standpipe to this drainage layer enabled the water table in the model to be controlled at a level 5mm below the retained ground level throughout the test. The sample was subjected to a preconsolidation pressure of 500kPa followed by swelling to 250kPa and was used for all tests to provide an overconsolidated sample prior to model making and spinning on the centrifuge. The distribution of pore pressure throughout the model was measured and the consequent theoretical vertical and horizontal total and effective stresses were therefore also known from simple calculations.

A cross section of the general model apparatus is shown in Figure 4. The mechanical apparatus essentially consisted of a manifold containing three hydraulic cylinders that were used to place successive levels of stiff walings against the retaining wall. Each hydraulic cylinder was actuated independently by means of motorised valves connected to a pressurised oil reservoir machined into the manifold. The reservoir became pressurised

under the enhanced self weight of a phosphor bronze piston. This heavy weight acting on the oil was capable of generating approximately 8 bar when in the centrifuge at 100g. Oil pressure in the hydraulic system was measured via three Druck 810 pressure transducers mounted within a specially manufactured block bolted to the manifold. This arrangement allowed for prop loads to be determined from changes in oil pressure resulting from movements of the retaining wall.

The presence of the walings and the practical difficulties of in-flight excavation made it necessary to form the excavated soil profile prior to spin up on the centrifuge. Reasonable distributions of correct pre-excavation vertical and horizontal stresses were independently maintained at the excavation boundaries using fluid pressures applied against the retaining wall and the excavation formation, the former provided by a heavy fluid contained by a polyethylene bag and the latter compressed air in a rubber bag. In order to simulate the reduction of stresses associated with the excavation these fluid pressures were reduced incrementally and in sequence with the installation of the three levels of propping. A solenoid valve was used to drain the dense fluid that was used to maintain the horizontal total stress whilst air pressure at excavation formation level was gradually reduced. The approach thus offered the opportunity to model separately the calculated horizontal and vertical total stresses acting against the retaining wall and the excavation formation level. The bags were separated by a stainless steel plate that was bolted to the underside of the hydraulic cylinder manifold. The plate therefore acted as a cantilever that was capable of providing restraint against the greater horizontal pressure applied by the dense fluid at the

junction of the retaining wall and formation level. A 2mm gap between the plate and the retaining wall was sufficient to maintain separation between the two membranes without imposing restraint to the wall at formation level.

The model wall had a flexural stiffness corresponding to a prototype concrete wall approximately 1.35m thick. A very stiff wall was used to minimise horizontal displacements caused by bending. The wall was manufactured from 10mm thick aluminium plate (Figure 5) and was sealed against the back wall of the strongbox and the Perspex window using cast silicone rubber seals⁽⁵⁾(Figure 6). Clearly, to ensure that a good seal could be maintained between the retaining wall and the strongbox there must be effective contact but with minimal friction to avoid unrepresentative restraint to the wall. With this in mind the overall width of the wall, including the seals, was 202mm. This was slightly greater than the width of the strongbox (200mm) and with provision for silicone grease to be applied to a recess formed in the surface of the soft cast silicone rubber. The purpose of this was to minimise friction whilst maintaining the water retaining effects (which was important owing to the fact that a water table was maintained just below the retained ground surface by means of a standpipe connected to the base of the model where there are drainage channels in contact with a porous plastic filter).

Owing to the requirement to maintain stiffness throughout the propping system, walings having a stiffness equivalent to that of a reinforced concrete slab of a realistic prototype

thickness of 300mm were manufactured. To calculate the equivalent stiffness the following assumptions were made:

- i) Top down flat slab construction incorporating 300mm thick rc slab.
- ii) Young's modulus for concrete $E_c = 25\text{kN/mm}^2$.
- iii) Load from earth pressure spreads through the retaining wall and slab at 45° giving an effective deep beam depth of 9.2m.

Hence, the stiffness $E_c I = 25 \times 10^6 \times \frac{0.3 \times 9.2^3}{12} = 486.7 \times 10^6 \text{ kNm}^2$

A beam of similar stiffness made from aluminium ($E_a = 70\text{kN/mm}^2$) required $I = 6.95\text{m}^4$. The profile adopted had $I = 7.45\text{m}^4$ at prototype scale and could therefore be regarded as very stiff. No attempt was made to model the prototype axial stiffness as this would be heavily dependent on geometry. The area of contact between the model waling and the retaining wall was limited to a 3mm wide nib that protruded 1.5mm beyond the waling flange. The nib therefore acted through the 500 gauge polyethylene membrane which inevitably reduced the stiffness of the propping system slightly.

CENTRIFUGE MODELLING PROCEDURE

Three sets of tests were carried out, the details of which are given in Table 1. Two sets of tests in which varying concentrations of piles were used at excavation formation level (AM13 and AM15) were compared with a test in which no piles were used (AM14). An embedded pile length of 120mm, equal to the depth of the excavation, was used since this would allow a thick layer of clay between the toe of the piles and the base of the model. A fairly arbitrary, but nonetheless realistic, pile layout was eventually adopted since it was assumed that the piles would provide a general stiffening effect to the formation rather than acting purely in tension and thereby anchoring down the excavated surface (Figure 7). This was consistent with the primary purpose of the piles being to reduce deep seated movements which would extend well beyond the depth of any piles that could be used in the model.

A “fast cast” resin, used commercially for complex and rotational mouldings, was used for the model piles. This product consisted of two parts that were separately mixed first with aluminium trihydrate (ON) filler, and then together, to form a pourable fluid with a pot life of about 2 minutes whilst curing would take about 20 minutes. Heat was generated during curing and was measured with a temperature sensor embedded in a pile hole but was found to be minimal. The pile holes were formed using a thin walled hypodermic steel tube inserted through a template simulating a pile bored by shell.

A series of tensile and compressive tests was subsequently carried out on samples of resin obtained from piles cast in a typical test. Difficulties existed over determining the most appropriate mode of testing since the piles may be subjected partially to tension but also to bending. However, the simple tests that could be performed on tensile and compressive specimens were thought adequate. The samples were tested well beyond the maximum strain that they may have been expected to achieve and from the graph shown in Figure 8 the stiffness, E_p , was determined to be approximately 800MPa. This value is less than might be expected for a concrete pile but still much stiffer than the model soil in which the model pile was placed. Furthermore, the density of the pile material was found to be about 1200kg/m^3 , about half of the density that could be assumed for concrete, but it was nonetheless still considered appropriate to use such a light weight material. This was because piles formed from the material could not provide any support to the excavation formation as a result of their self weight and therefore any reduction in displacements in tests with piles could be assumed to be as a result of stiffening effects only.

Black plastic marker beads were pressed into the vertical surface of the soil, generally on a 10mm grid, to enable displacements to be measured throughout the model using image processing techniques. When the apparatus had been placed and fixed into position the Perspex window, which also incorporated the image measurement system control targets, was bolted in place. The window was first lubricated using a high viscosity, clear, silicone oil. A rack containing standard displacement transducers, LVDTs (linearly variable differential transformers), to record vertical displacements of the ground surface behind the

retaining wall as well as providing a means of direct measurement of wall rotation, was bolted on top of the strongbox (Figure 9).

In the first phase of the centrifuge test the model underwent a period of consolidation under its enhanced self weight at 100g. This resulted in additional swelling throughout the depth of the model as effective stress equilibrium was established. The time taken for this was usually about 36 hours.

Since the vertical total stress at the excavation formation level was maintained and controlled using a rubber bag supplied with compressed air it was necessary, during spin-up, to increase the pressure incrementally with the centrifuge speed. This ensured that the vertical and horizontal total stresses were in the correct ratio at all times. Whilst the required pressure in the rubber bag could be determined easily the fluid density in the polyethylene bag was more difficult to match to the horizontal stress expected owing to the non-linear variation of stress with depth. Zinc iodide solution mixed to a specific gravity of 1.91 was used to give a hydrostatic pressure of 228kPa acting horizontally at excavation formation level. This required pressure was calculated assuming a saturated bulk unit weight for the kaolin of 17.44kN/m^3 , an average K_0 of 1.2 and that the pore water pressure was hydrostatic with the water table 5mm below the top surface of the model. The imposed fluid restraint proved to be approximately correct as movement of the wall during consolidation on the centrifuge was barely detectable.

When the model reached a speed giving an acceleration of 100g it was left rotating at that speed, at least overnight but more often for about 30 hours, for the pore pressures to come into equilibrium whereupon the following excavation test procedure was carried out:

- i Advance top prop and lock into position.
- ii Drain heavy fluid to level of middle prop whilst simultaneously reducing air pressure at formation to suit rate of drainage. (Stage 1 excavation).
- iii Advance middle prop and lock into position
- iv Drain heavy fluid to level of bottom prop whilst simultaneously reducing air pressure at formation to suit rate of drainage. (Stage 2 excavation).
- v Advance bottom prop and lock into position.
- vi Drain remainder of heavy fluid whilst simultaneously reducing air pressure at formation to suit rate of drainage. (Stage 3 excavation).

The duration of this excavation phase was mainly controlled by the rate of fluid drainage and the air pressure was manually adjusted to maintain the vertical total stress acting at formation consistent with the simulated unexcavated height of soil.

DISPLACEMENT MEASUREMENT USING DIGITAL IMAGE ANALYSIS

Digital image analysis enables displacements throughout the model to be tracked using photogrammetry techniques. The image processing system used in conjunction with these tests was developed as a joint research project with the Engineering Surveying Research Centre at City University and is described in detail by others^{6,7}. The system relies on the capture of images using CCD (charge coupled device) cameras and tracking the movement of targets in the image plane recorded on the pixel board of the camera. For the tests reported the video output from two CCD cameras was relayed through the slip rings. Each camera was connected to a PC with a frame grabber card and discrete images were grabbed and stored at 2 second intervals during, and for the period immediately after, the simulated excavation stage of the test. The mathematics associated with the close range photogrammetry is beyond the scope of this paper but information on the background is given by Cooper and Robson⁸. The distortion resulting from the camera and camera position are calibrated out, as is the refractive index of the 80mm thick perspex window through which the model is viewed. A series of targets, known as 'control targets', that are etched into the perspex at known positions, are used for this purpose. The system is capable of measuring to an accuracy of about $\pm 25\mu\text{m}$ which for a model tested at 100g is equivalent to $\pm 2.5\text{mm}$ at prototype scale.

TEST RESULTS

The results of three tests are reported in this paper, the details being summarised in Table 1. The method of propping used in the tests was intended to be as stiff as possible such that displacements resulting from horizontal movement of the wall were minimised. However, the system was less stiff than had been intended, owing to difficulties with removing air entirely from the hydraulic system, and this led to larger vertical displacements behind the retaining wall than would be expected in a comparable prototype. Clearly, the magnitude of horizontal displacements was consequently greater than could be reasonably expected at prototype scale but the influence of the piles in reducing these movements, as well as the total prop load, was nonetheless clear.

Displacements

The excavation formation was subjected to large reductions in vertical stress during the simulated excavation in the centrifuge tests. This was characterised by the generation of significant negative excess pore pressure in the soil immediately beneath the excavation; the magnitude of change in pore pressure decreased with increasing distance from the unloaded surface. Typical pore pressure responses during the simulated excavation stage of test AM13 are shown in Figure 10. These pore pressure responses confirm that whilst the major changes in stress occurred beneath the excavation there was also significant horizontal unloading as shown in the response of ppt2, ppt3 and ppt4.

In Figure 11 image processing data from a row of markers placed 5mm below formation level have been used to measure the development of heave in test AM14 at key stages of the simulated excavation. The response to the unloading caused by excavation was non linear, with an initially small, possibly elastic heave displacement at formation level. This heave increased steadily as total vertical stress, σ_v was gradually reduced by decreasing the air pressure acting at excavation formation level. Quite a large variation in displacement over the width of the excavation was evident by the time the simulated excavation was complete with the greatest movement occurring near to the retaining wall. The magnitude of heave in this area was probably influenced by displacement of the toe of the retaining wall towards the excavation whereas near to the end wall of the strongbox reduced displacement in comparison to the area near to the retaining wall, at this relatively early stage, might have resulted from boundary effects such as excessive friction against the end wall of the strongbox.

Two of the image processing targets, placed 5mm below the excavation formation level, have been used to represent the range of displacements shown in Figure 12. The two targets depict the maximum and minimum heave displacements plotted on Figure 11 (i.e. the targets positioned at 25mm and 130mm from the retaining wall). Displacements measured during the first two stages of excavation constituted only 25% or less of the total movement generated at the completion of the simulated excavation whilst a significant increase in the rate of displacement accompanied the final stage of unloading. This is because, during the early stages of excavation the soil strength is mobilised and the soil

immediately below the excavation largely resists the heave. However, as the excavation progresses and approaches the final stage, plastic straining begins and spreads through the soil mass immediately below the excavation. A state of passive failure is reached when the soil strength is mobilised over the embedded depth of the wall.

After excavation was complete and with increasing time, further plastic straining at greater depths below formation level led to mobilisation of soil strength over an enlarged perimeter of soil around the base of the excavation. This contributed to overall stability beneath the excavation and resulted in a reduction in the rate of movement but not to its cessation. As there is no load change, owing to completion of the simulated excavation, there should be no further movement at the base of the excavation unless another process is active. The continued heave is caused by water, supplied from the base drain, seeping towards the excavation resulting in further plastic straining associated with softening. The behaviour described is shown in Figure 13 in which contours of vertical displacement at three stages (end of excavation, 15 minutes and 30 minutes after excavation completed where 1 minute \approx 1 week at prototype scale) of test AM14 are shown depicting the soil response due to the unloading caused by excavation. Very small movements resulted from excavation alone but after 15 minutes there is a spread of movement throughout the soil beneath the excavation and behind the retaining wall. After a further 15 minutes there is only significant additional movement in the soil immediately below the formation. This clearly suggests time dependent dissipation of excess pore water pressure due to the stress changes caused by the simulated excavation. The changes in pore water pressure contribute to both

a reduction in shear strength and swelling of the clay although it is not possible to distinguish between these two effects.

At the retained ground surface settlements were influenced by both the unloading at formation level and also any flexibility that existed in the wall and propping system. The propping was found to be less stiff than had been intended, owing to a small amount of air trapped in the hydraulic system, and this led to increased settlement. However, some wall movement is beneficial since this tends to amplify the effects of stiffening the excavation formation, thereby demonstrating that the use of piles could mitigate against any lack of stiffness in the propping system.

Substantially more settlement near to the retaining wall was observed in test AM14 (Figure 16) in which no piles were installed at formation level and successive reductions in displacement accompanied the introduction of one and two rows of piles. Reductions in maximum settlement of approximately 40% and 55% are seen near to the retaining wall with one and two rows of piles, respectively, but this effect reduces fairly sharply at greater distances from the excavation.

The manner in which settlement behind the retaining wall was reduced is significant since the greatest reduction in magnitude of displacement tends to coincide with the position of maximum displacement for an unstiffened formation. This is shown in Figure 16. In all tests this occurred consistently at a distance of $0.5H$ behind the retaining wall. Such

localised reduction in the settlement trough has obvious potential for avoiding the notoriously damaging angular distortions associated with differential settlement. Further away from the retaining wall, at distances beyond about 2H, it appears that the use of piles did not affect the magnitude of settlement to any discernible extent.

Prop Loads

In Figure 14 the gradual reduction in fluid pressure providing support to the retaining wall during the tests is depicted by a blue line.

The ordinate $\frac{\Sigma P + \frac{1}{2} \gamma h_f^2 w}{\frac{1}{2} \gamma H^2 w}$

is the sum of the total prop load, ΣP , and the load from the dense fluid acting during the excavation sequence, $\frac{1}{2} \gamma h_f^2 w$, normalised by the total fluid pressure prior to excavation commencing. Immediately before the top prop was installed the total prop load, ΣP , was zero, no fluid had been drained and the expression reduces to unity. Therefore unity on the ordinate represents the normalised total lateral load acting on the retaining wall during the period of reconsolidation prior to the simulated excavation. Installation of the top prop prior to draining any fluid increased the value on the ordinate to about 1.5 in all tests. As the fluid drained during the first stage of the excavation the prop loads remained fairly constant and by the end of this stage the normalised support pressure from props and fluid was slightly less than unity. This means that the total lateral support was fractionally less than that provided throughout the period of reconsolidation. The two subsequent levels of prop installation however restored and increased the support pressure to a value equal to

about twice the original fluid pressure upon completion of the excavations in which piles were used and to about three times the original fluid pressure where no piles were used. Thereafter, in all tests, the total prop load continued to rise as excess pore pressures in the vicinity of the retaining wall dissipated. The development of support pressure suggests that the propping system was, for the greater part of the excavation sequence, subjected to forces in excess of the fluid pressure used to support the retaining wall during reconsolidation, implying a reasonably stiff propping system. However, it is significant that the total propping force in the tests with piles was substantially less than for the test with no piles in the formation.

Image processing data indicate that there was noticeable horizontal movement during the simulated excavation suggesting possibly low initial stiffness in the propping system. This means that the toe of the retaining wall could be expected to rely on the soil below excavation formation level to generate a certain amount of passive resistance, the magnitude of which was determined by the effectiveness of the propping. Mobilisation of passive resistance would vary inversely with increasing prop stiffness. However, the ability to provide such passive support reduces with time following the simulated excavation especially as the imposed groundwater regime (maintained at 5mm below the retained ground surface) subjected the soil around the base of the excavation to quite high pore pressures. Any softening would clearly reduce the maximum available passive resistance.

The stiffening influence of piles is apparent from image processing data of horizontal displacements 5mm behind the retaining wall (Figure 15) at the completion of the simulated excavation. The stiffness of the propping system was unaltered in the three tests considered, suggesting that the use of one row of piles led to approximately 50% reduction in horizontal movement whereas two rows of piles reduced the movement to about 30% of that measured in the tests without piles. Such reductions, although quite large, correlate well with those seen for settlement behind the retaining wall (Figure 16).

The strong influence of piles on horizontal displacement would be expected to be reflected, to some extent, in the measured prop forces since similar total horizontal forces could be expected in all tests. In order to provide an indication of this the development of prop loads during the simulated excavation stage of the tests is shown in Figure 17. The reduction in total prop force with the introduction of successive rows of piles is clear. With one row of piles the total prop force was reduced by about 30% and further reduction is indicated in test AM13 in which an additional row of piles was installed. Problems with a partially blocked drainage pipe during test AM13 meant that the time taken to complete the simulated excavation stage was longer in this test and it therefore seems likely that the magnitude of prop force is over estimated in relation to tests AM14 and AM15, although the trend of reducing prop loads with increasing use of piles at excavation formation level is nonetheless evident.

CONCLUSIONS

The behaviour seen in the centrifuge tests has been remarkably consistent and allows a number of statements to be made concerning the effects of cast in situ piles used to enhance the stiffness of the ground below excavation formation level in propped excavations.

The maximum settlement behind the retaining wall occurs at a distance of $0.5H$, where H is the depth of excavation, and significant displacements are apparent within the retained soil, up to a horizontal distance of $3H$ behind the retaining wall. The influence of piles on settlement is limited to a distance of about $2H$. Magnitudes of displacement are highly dependent upon the current depth of excavation with much increased movements accompanying the deepest levels of excavation. Only 25% or less of overall displacement was seen to occur as a result of the first two stages of excavation whilst the remaining 75% of displacement was associated with the last 40% of excavation. The proportions of movement associated with each stage of excavation were not influenced by the introduction of piles at excavation formation level.

Whilst the propping system in the apparatus may not have been as stiff as a realistic equivalent prototype the series of tests confirms that piles can be used as a means of reducing ground movement around deep excavations. Importantly, the test results have emphasised the influence of formation stiffness on all movements. The piles have been

found to work in two ways that combine to reduce both vertical displacements at the retained ground surface and horizontal displacements behind the retaining wall.

The piles appear to work in tension over their embedded length to reduce heave at the base of the excavation when it is subjected to vertical unloading caused by removal of the overburden during excavation ; in addition they provide a stiffening effect to the soil in the passive zone by acting in bending, thereby reducing horizontal wall movement and prop loads. These effects may well be underestimated in comparison to the equivalent prototype concrete piles which were relatively stiffer.

The reduction in heave at formation level, with the use of piles, has been found to correlate well with a similarly reduced magnitude of settlement at the retained ground surface as well as horizontal displacement behind the retaining wall over the period considered. The use of an additional row of piles enhances the stiffening effects seen with a single row of piles although the further benefit accruing is not of the same magnitude.

REFERENCES

1. McNamara, A.: *Influence of heave reducing piles on ground movements around excavations*, PhD Thesis, City University, 2000.
2. Schofield, AN.: *Cambridge geotechnical centrifuge operations*, *Geotechnique* **30**, No.3, pp227-268, 1980.
3. Taylor, RN: *Centrifuges in modelling: Principles and scale effects*. Geotechnical centrifuge technology, Blackie Academic and Professional, Taylor, RN (Ed) Glasgow, pp19-33, 1995.
4. Schofield, AN. and Taylor, RN.: *Development of standard geotechnical centrifuge operations*. Centrifuge 88, Ed Corté, Balkema, Rotterdam, 1988.
5. Powrie, W.: *The behaviour of diaphragm walls in clay*, PhD Thesis, University of Cambridge, 1986.
6. Taylor, RN. Grant, RJ. Robson. S. Kuwano, J.: *An image analysis system for determining plane and 3-D displacements in soil models*. Centrifuge 98, Kimura, Kusakabe and Takemura (Eds), Balkema, Rotterdam, 1998.
7. Grant, RJ.: *Movement around a tunnel in two-layer ground*. PhD Thesis, City University, 1998.

Test Reference	Date of test	Retaining Wall Height (mm)	Retaining Wall Embedment (mm)	Number of Levels of Props	Number of rows of piles	Total Number of Piles
AM13	23/11/99	120	40	3	2	10
AM14	14/12/99	120	40	3	0	0
AM15	28/1/00	120	40	3	1	5

Table 1 Summary of parameters for tests reported.

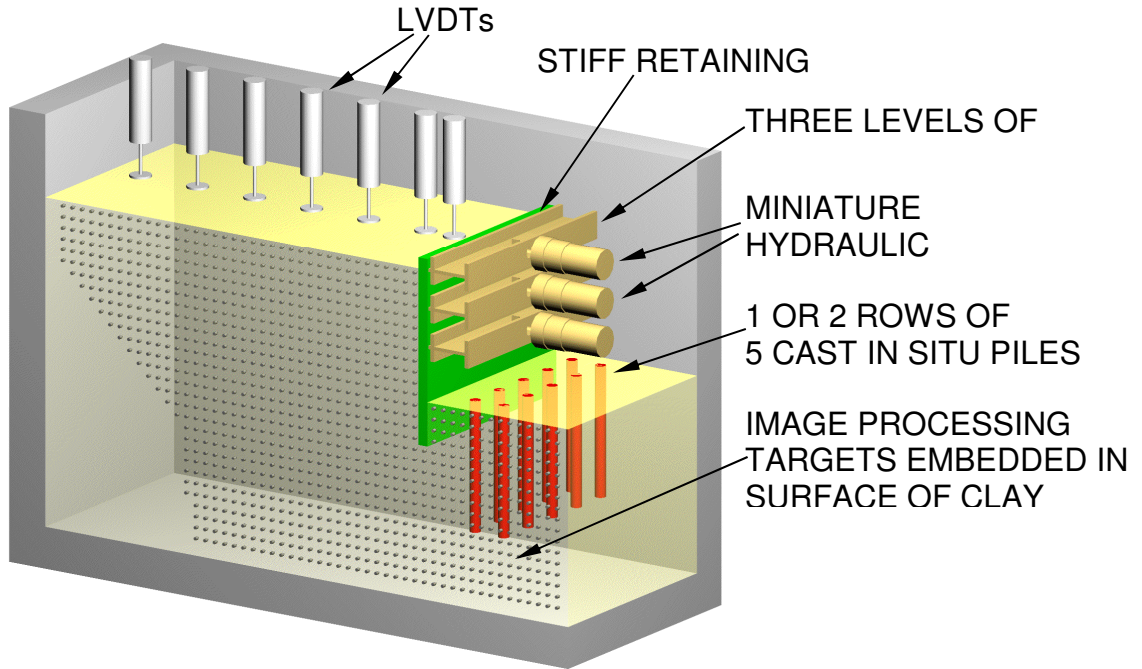


Figure 1 Schematic view of the model showing key components of the apparatus for modelling top down construction.

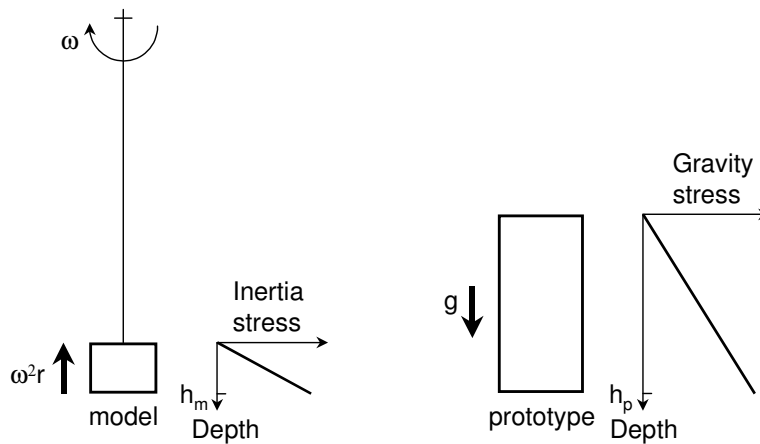


Figure 2 Inertial stresses in a centrifuge model compared with gravitational stresses in a corresponding prototype (after Taylor 1995)

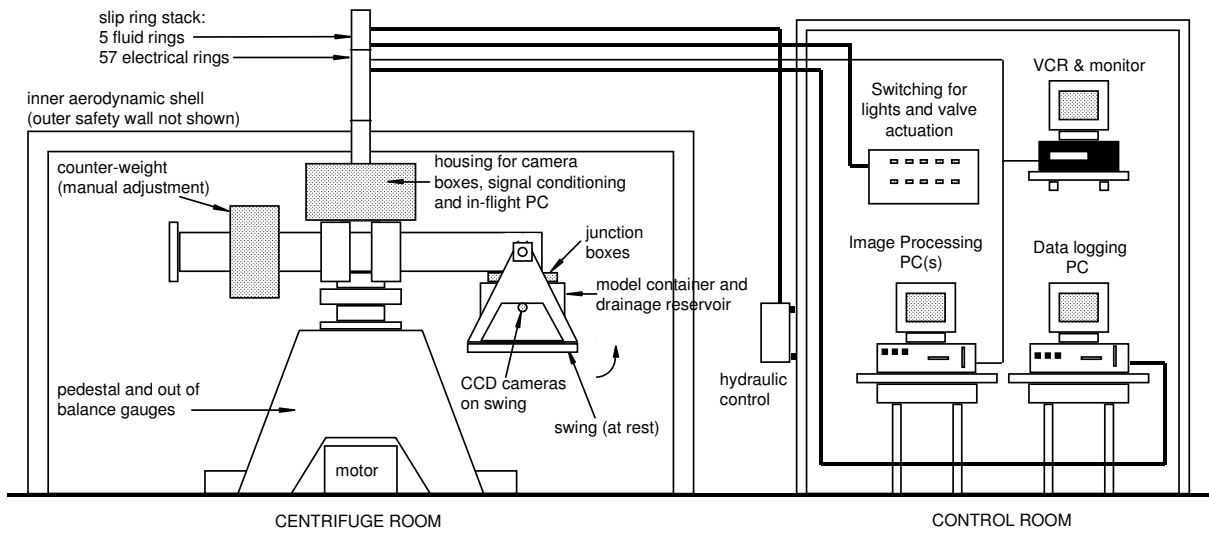


Figure 3 Schematic diagram of the Acutronic 661 geotechnical testing facility at City University, London. (after Grant 1998)

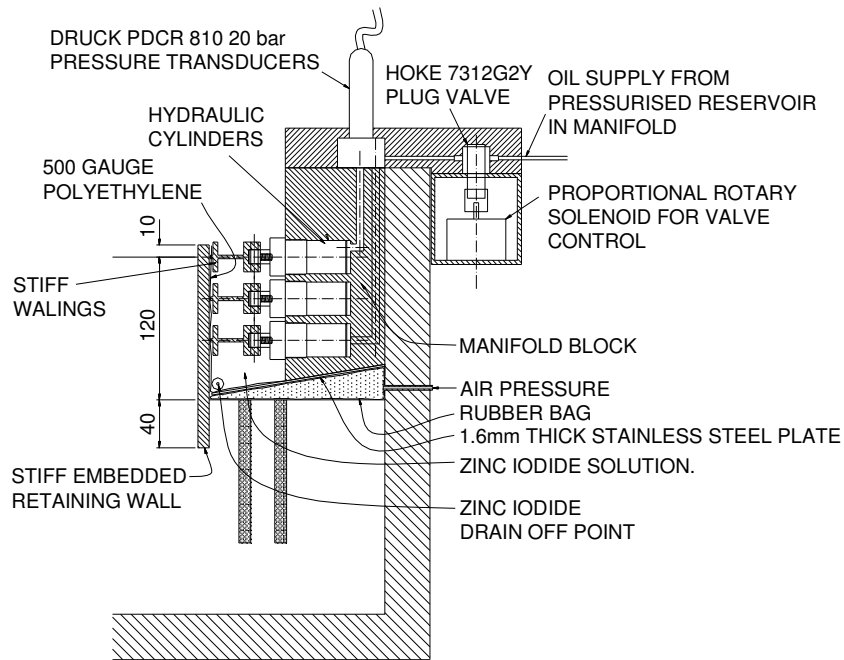


Figure 4 General arrangement of main apparatus

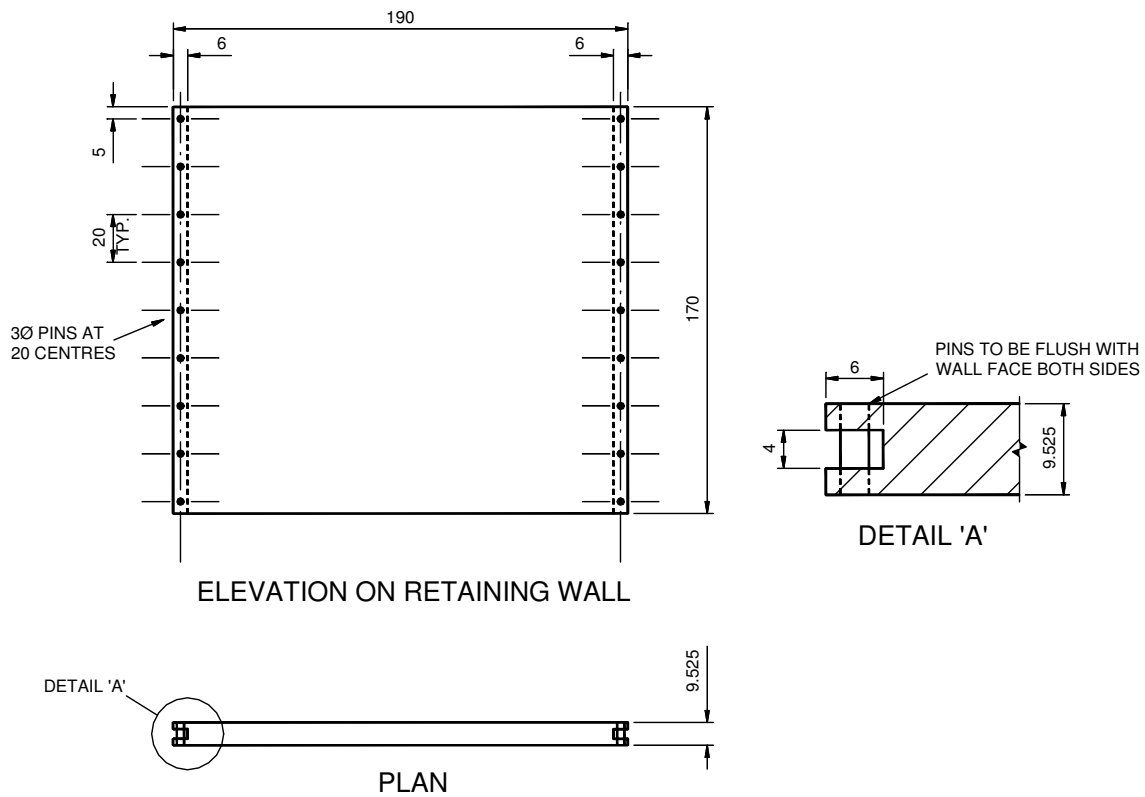


Figure 5 Details of model retaining wall and method of securing cast silicone rubber seals into rebates

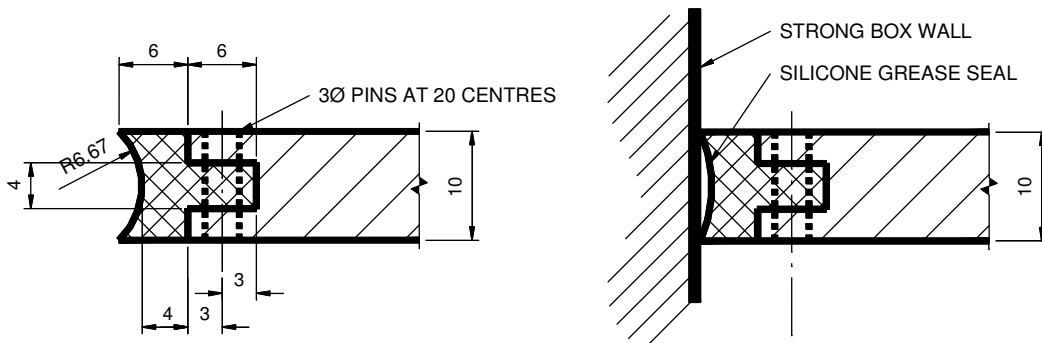


Figure 6 Detail of cast silicone rubber seal in model retaining wall and against strongbox wall

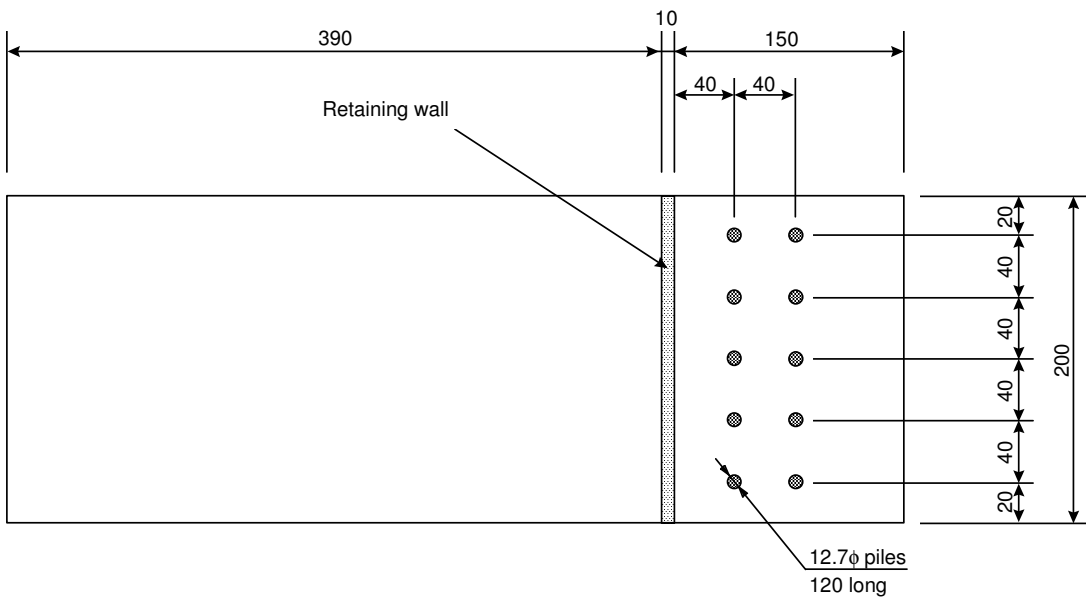


Figure 7 Layout of piles. Either one or two rows of piles were used for tests in which the excavation formation was stiffened. The line of piles nearest to the retaining wall was used for tests with one row.

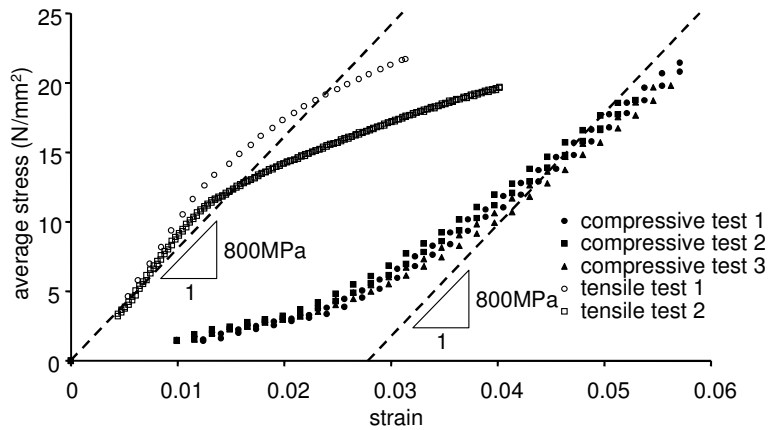


Figure 8 Comparison of tensile and compressive tests on piles made from Sika Biresin G27 mixed 50:50 w/w with aluminium trihydrate (ON) filler.

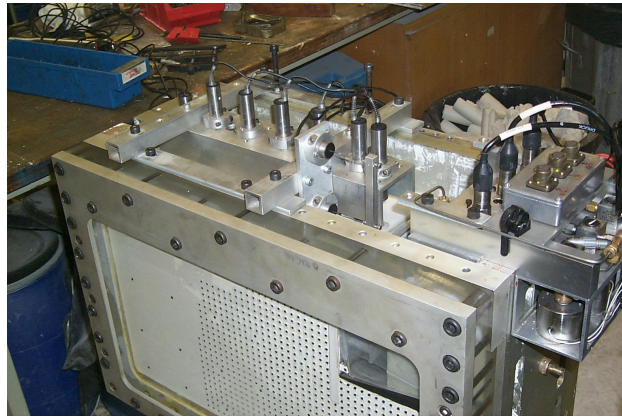


Figure 9 Completed centrifuge model ready for testing

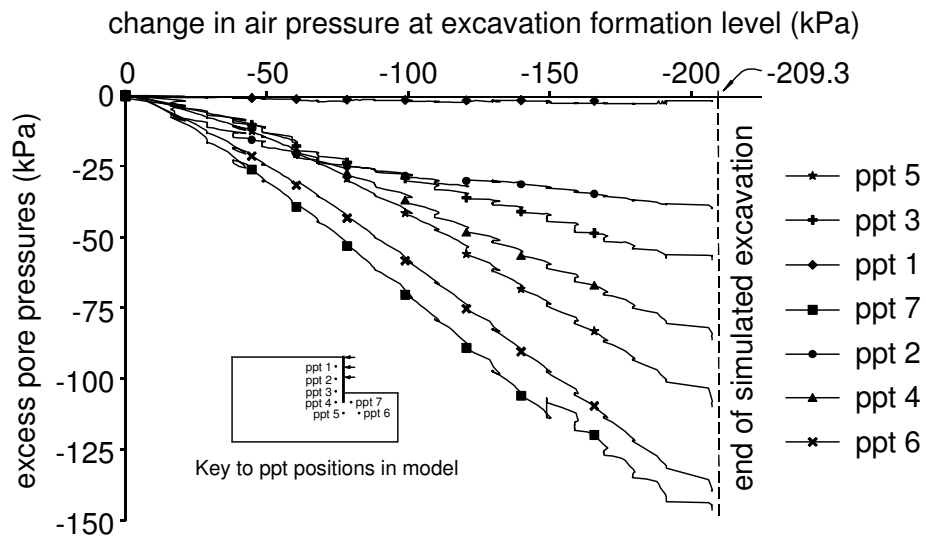


Figure 10 Generation of excess pore pressures during the simulated excavation stage of a typical test.

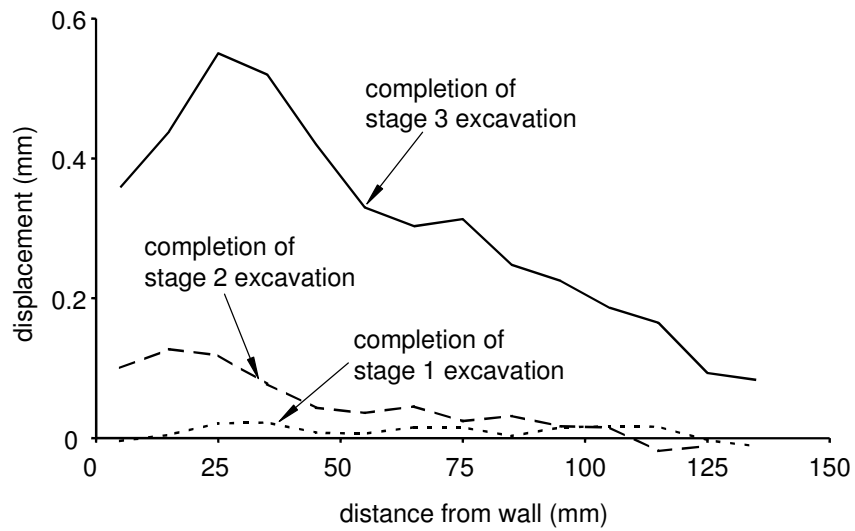


Figure 11 Deformation of excavation formation during the simulated excavation stage of a typical test.

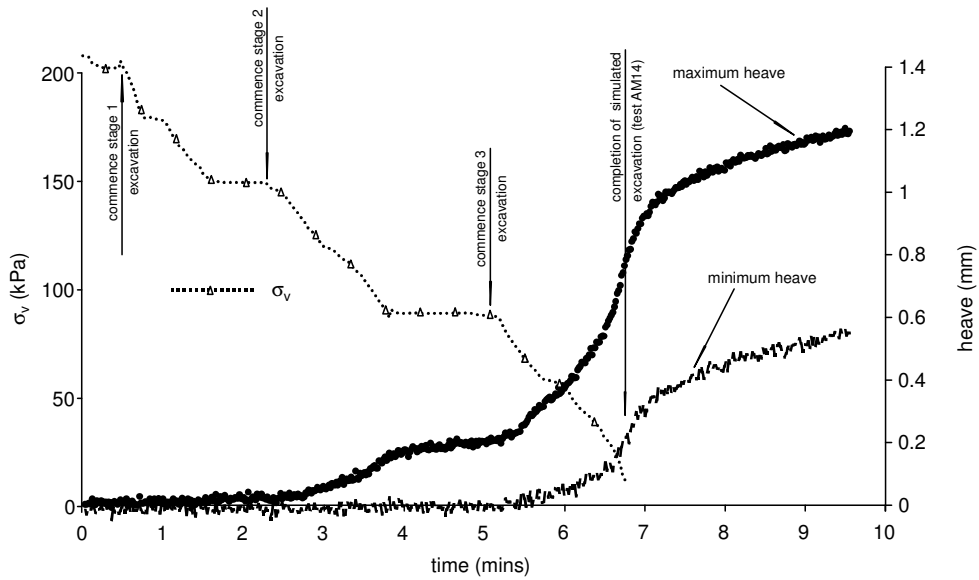
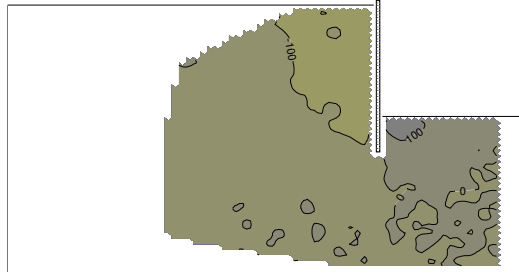
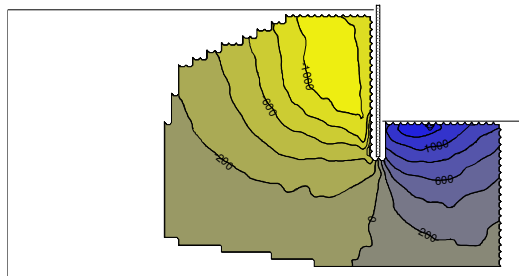


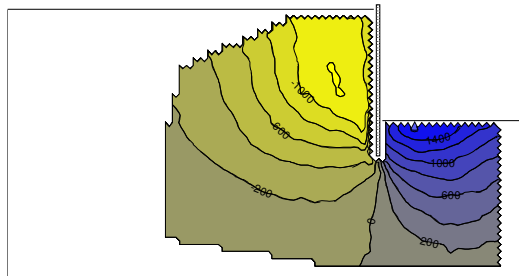
Figure 12 Development of heave displacements during simulated excavation in test AM14.



- a) At completion of simulated excavation. A small amount of heave is well established over a substantial depth beneath the excavation.



- b) After 15 minutes. Softening at formation level has resulted in large increases in heave in front of the retaining wall toe. Displacements at ground level have increased dramatically.



- c) After 30 minutes. Heave and settlements have increased but at a much reduced rate owing to the fact that there is no load change and the soil at formation level is softening.

Figure 13 Contours of vertical displacement at key stages during test AM14 (displacements in µm)

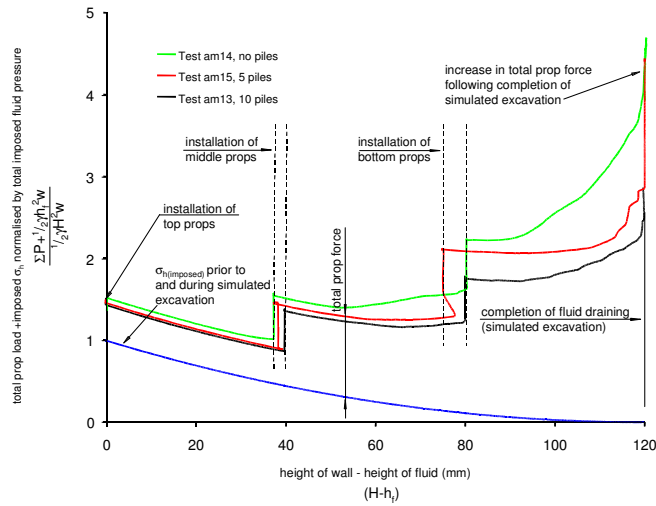


Figure 14 Variation of total retaining wall support pressure normalised by total imposed fluid pressure with reduction in height of fluid for all tests. Also shown, to demonstrate the development of the total prop force, is the reduction in fluid pressure during the simulated excavation stage of the test.

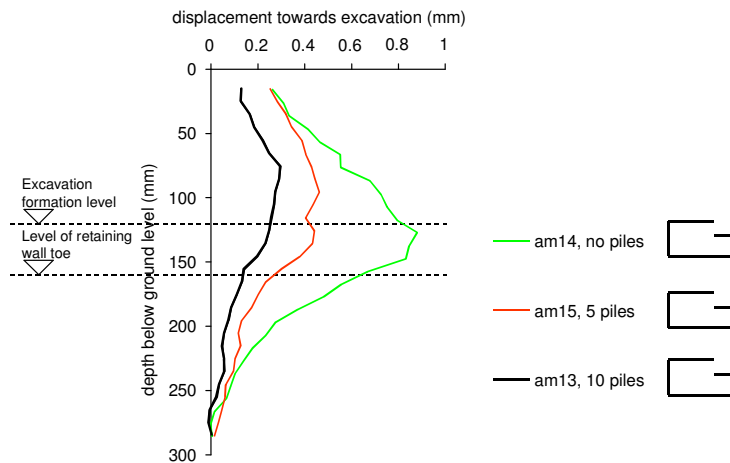


Figure 15 Comparison of horizontal displacements behind the retaining wall measured using image processing at completion of the simulated excavation stage of all tests.

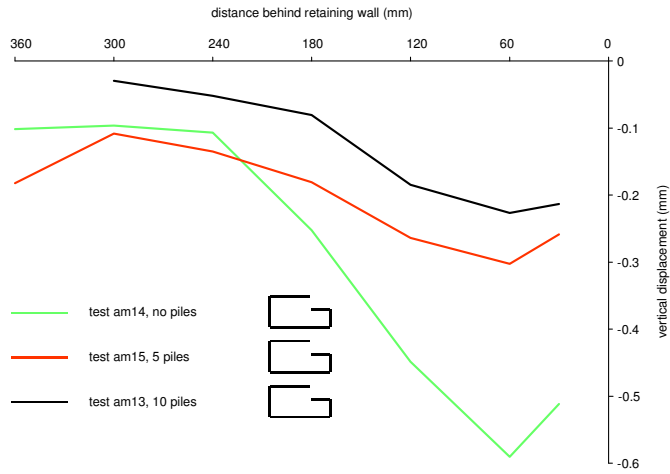


Figure 16 Comparison of approximate retained surface settlements attributable to horizontal movement of the retaining wall at the end of the simulated excavation stage of typical tests.

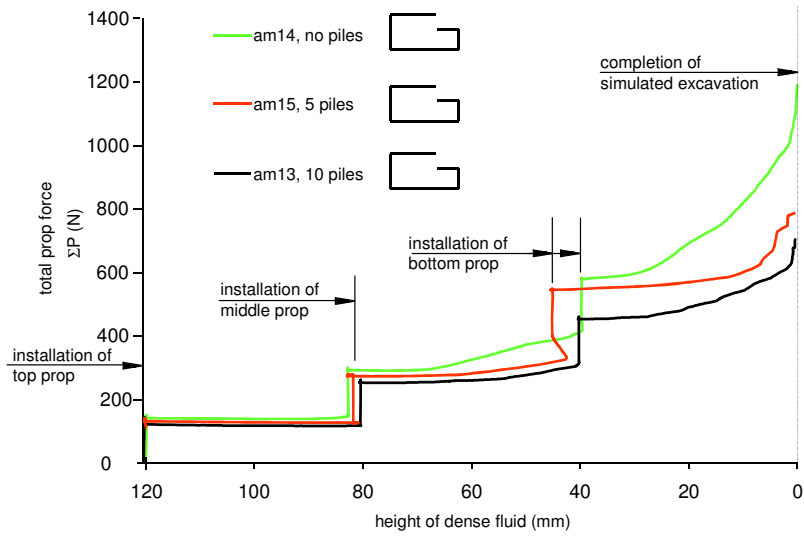


Figure 17 Comparison of development of total prop force during simulated excavation in all tests.